

Do Cortical Neurons Process Luminance or Contrast to Encode Surface Properties?

Tony Vladusich, Marcel P. Lucassen and Frans W. Cornelissen

JN 95:2638-2649, 2006. First published Dec 28, 2005; doi:10.1152/jn.01016.2005

You might find this additional information useful...

This article cites 61 articles, 24 of which you can access free at:

<http://jn.physiology.org/cgi/content/full/95/4/2638#BIBL>

Updated information and services including high-resolution figures, can be found at:

<http://jn.physiology.org/cgi/content/full/95/4/2638>

Additional material and information about *Journal of Neurophysiology* can be found at:

<http://www.the-aps.org/publications/jn>

This information is current as of April 7, 2006 .

Do Cortical Neurons Process Luminance or Contrast to Encode Surface Properties?

Tony Vladusich,¹ Marcel P. Lucassen,² and Frans W. Cornelissen¹

¹Laboratory of Experimental Ophthalmology and NeuroImaging Centre, School of Behavioural and Cognitive Neurosciences, University Medical Centre Groningen, University of Groningen, Groningen; and ²Department of Human Interfaces, Netherlands Organization for Applied Scientific Research–Human Factors, Soesterberg, The Netherlands

Submitted 27 September 2005; accepted in final form 25 December 2005

Vladusich, Tony, Marcel P. Lucassen, and Frans W. Cornelissen.

Do cortical neurons process luminance or contrast to encode surface properties? *J Neurophysiol* 95: 2638–2649, 2006. First published December 28, 2005; doi:10.1152/jn.01016.2005. On the one hand, contrast signals provide information about surface properties, such as reflectance, and patchy illumination conditions, such as shadows. On the other hand, processing of luminance signals may provide information about global light levels, such as the difference between sunny and cloudy days. We devised models of contrast and luminance processing, using principles of logarithmic signal coding and half-wave rectification. We fit each model to individual response profiles obtained from 67 surface-responsive macaque V1 neurons in a center-surround paradigm similar to those used in human psychophysical studies. The most general forms of the luminance and contrast models explained, on average, 73 and 87% of the response variance over the sample population, respectively. We used a statistical technique, known as Akaike's information criterion, to quantify goodness of fit relative to number of model parameters, giving the relative probability of each model being correct. Luminance models, having fewer parameters than contrast models, performed substantially better in the vast majority of neurons, whereas contrast models performed similarly well in only a small minority of neurons. These results suggest that the processing of local and mean scene luminance predominates over contrast integration in surface-responsive neurons of the primary visual cortex. The sluggish dynamics of luminance-related cortical activity may provide a neural basis for the recent psychophysical demonstration that luminance information dominates brightness perception at low temporal frequencies.

INTRODUCTION

How does the brain transform light signals registered on the retina into visual surface representations? Classical psychophysical studies of brightness and color constancy imply that surface representations are formed through the long-range spatial integration of visual information (Land 1959, 1977, 1983, 1986). One version of the well-known retinex model (Land and McCann 1971), for example, posits that the brain spatially integrates the contrasts, or log luminance ratios, formed at reflectance borders, to discount global illumination conditions. Related computational approaches advocate the filling-in of contrast information within the regions defined by object boundaries (Cohen and Grossberg 1984; Gerrits and Vendrik 1970; Grossberg and Todorovic 1988), a process that

is generally assumed to occur in the visual cortex (Grossberg and Mingolla 1985; Komatsu et al. 2000, 2002; Pessoa et al. 1998). Recent psychophysical studies, however, have shown that the tendency toward brightness constancy can be relatively weak (Masin 2003), even in complex displays (Arend and Spehar 1993a,b; Robilotto and Zaidi 2004). Furthermore, classical experiments with Ganzfeld stimuli indicate that human observers can act like photometers in the absence of contrast information (Barlow and Verrillo 1976). These psychophysical findings are consistent with the informal observation that humans are easily able to perceive global illumination changes, such as when a cloud passes overhead. It is important to note, however, that the scaling of local luminance to mean scene luminance has been proposed as a mechanism to underlie the tendency toward brightness constancy (Helson and Himelstein 1955; Robilotto and Zaidi 2004). In summary, understanding the roles of contrast and luminance processing may shed light on the nature of the cortical computations underlying surface perception.

How do the concepts of contrast and luminance processing compare with neurophysiological data? The center-surround properties of receptive fields (RFs) in the mammalian retina and lateral geniculate nucleus (LGN) are generally taken as evidence that early visual processes transmit contrast information, rather than luminance information, to visual cortex. Indeed, the preponderance of contrast-responsive neurons in retina and LGN forms the basis for some general computational approaches to vision (Grossberg and Mingolla 1985). Evidence from the cat (e.g., Barlow and Levick 1969; Mante et al. 2005; Rossi and Paradiso 1999), however, shows that many retinal and LGN neurons encode luminance information, in addition to contrast information. In monkey primary visual cortex (V1), there is strong evidence that some neurons encode the luminance of Ganzfeld stimuli (Kayama et al. 1979; Maguire and Baizer 1982). Thus contrary to the textbook view, the neural building blocks for the processing of luminance information are clearly available in visual cortex of monkey and cat.

In visual cortex, the responses of a small proportion of neurons qualitatively mirror aspects of human brightness constancy (MacEvoy and Paradiso 2001), simultaneous brightness contrast (Kinoshita and Komatsu 2001; Rossi and Paradiso 1999; Rossi et al. 1996) and brightness filling-in (Hung et al. 2001; Komatsu et al. 2000; Roe et al. 2005). Some authors

Address for reprint requests and other correspondence: T. Vladusich, Laboratory of Experimental Ophthalmology and NeuroImaging Centre, School of Behavioural and Cognitive Neurosciences, University Medical Centre Groningen, University of Groningen, PO Box 30.001, Groningen 9700 RB, The Netherlands (E-mail: t.vladusich@med.umcg.nl).

The costs of publication of this article were defrayed in part by the payment of page charges. The article must therefore be hereby marked "advertisement" in accordance with 18 U.S.C. Section 1734 solely to indicate this fact.

have found that few neurons in cat striate cortex (Hung et al. 2001; MacEvoy and Paradiso 2001) and monkey V1 (Friedman et al. 2003) respond vigorously to changes in surface luminance that are unaccompanied by concurrent stimulation of the classical RF with contrast stimuli. The apparent sparsity of neurons sensitive to the properties of uniform surfaces has even led some authors to conclude that surface brightness and color are exclusively encoded by *border-responsive* neurons (Friedman et al. 2003; Zhou et al. 2000; see also Blakeslee and McCourt 1999). Kinoshita and Komatsu (2001) recently described *surface-responsive* neurons that integrate information over large regions of the visual field and respond vigorously to uniform surfaces in the absence of local-contrast changes, and in some cases even local-luminance changes, in the classical RF (see also Peng and Van Essen 2005; Roe et al. 2005).

Here we develop a detailed computational-statistical framework to *quantitatively* assess whether cortical neurons process luminance or contrast information. We demonstrate the utility of the framework by analyzing the data described in the Kinoshita and Komatsu (2001) study. Our approach combines elements familiar in the areas of computational vision modeling and model selection. First, we assume logarithmic processing of luminance and contrast signals (Barlow and Verrillo 1976; Land and McCann 1971). To a first approximation, logarithmic processing captures the highly nonlinear signal processing that occurs in the early visual pathway. Second, we implement half-wave rectified (HWR) processing on the inputs and outputs of modeled neurons, which captures the notion that neurons cannot generate negative spike rates (Grossberg and Mingolla 1985; Heeger 1993). Third, we apply a statistical technique (Burnham and Anderson 2002), known as Akaike's information criterion (AIC), to examine multiple versions of the contrast and luminance models. The AIC method trades off the number of free-model parameters against fit quality, thereby introducing the concept of parsimony into model analysis. The AIC approach also overcomes some known limitations to conventional statistical methods for analyzing model performance, allowing *batch analysis* of both nested and nonnested models (e.g., contrast vs. luminance) without the need to specify null hypotheses or make corrections for multiple comparisons.

METHODS

Kinoshita–Komatsu paradigm and classification scheme

Simulations were carried out on cells classified in the original publication of Kinoshita and Komatsu (2001). We first briefly describe the methods of this study. For details we refer to the original publication. Neuronal responses were recorded in two separate conditions. In one condition, the luminance of a central square, embedded in a background of constant luminance, was varied in seven equal log steps ranging from 0.1 cd/m² (candelas per square meter) to 100 cd/m². The size of the center stimulus was always much larger than the hand-mapped classical RF (which was itself often tuned to oriented stimuli). In a second condition, the luminance of an annulus surrounding the central stimulus was varied through the same range as that used for the center-change tests. In this case, both the central square and the background surface had constant luminance. Importantly, the luminances of the square and the background were tailored to optimally excite a given neuron. As such, the square and background luminances were generally different, meaning that for most neurons there was *always a border present in the image*. We note here

the similarity between the stimuli used in the Kinoshita–Komatsu study and those typically used in studies of human brightness perception (Arend and Spehar 1993a,b; Bindman and Chubb 2004a,b; Hong and Shevell 2004a,b; Reid and Shapley 1988; Rudd and Arrington 2001; Rudd and Zemach 2004; Shapley and Reid 1985; see also Boucard et al. 2005; Huang et al. 2002).

The raw data for each neuron were provided to us by the authors. The sample consisted of 67 single- and multiunit recordings (hereafter referred to as “neurons”) classified into six groups, according to their response profiles. The original data set included 76 neurons, but nine were excluded because they were not subjected to the same experimental conditions as the other neurons. One class of neurons (Bright Type 1) responded to increasing surface luminance with monotonic increases in firing rates, but were unaffected by changes in the luminance of the annulus surrounding the central surface. A second class of neurons (Bright Type 2) responded to changes in the luminance of the central square and of the annulus in a manner consistent with human brightness contrast. That is, these neurons increased their firing rates in response to increasing central-surface luminance but decreased their firing rates in response to increasing annulus luminance (in which case humans would perceive a darkening of the central surface). The third class (Bright Type 3) responded to increases in both central-surface and annulus luminances with increased firing rates. Kinoshita and Komatsu also described Dark-type neurons, with complementary response profiles to those of the Bright-type neurons.

The number of cells for each classification were: Bright Type 1 cells ($n = 13$), Bright Type 2 cells ($n = 14$), Bright Type 3 cells ($n = 22$), Dark Type 1 cells ($n = 5$), Dark Type 2 cells ($n = 11$), and Dark Type 3 cells ($n = 2$). These RF classifications were based on the slopes of the response functions, observed during the later part of the response phase. For most neurons, the recording phase was between 520 and 1,020 ms after stimulus onset (see DISCUSSION).

Half-wave rectified contrast model

We first specify the most general form of the contrast model and then derive two simpler forms that we also test. The contrast model is an adapted version of the retinex model (Land and McCann 1971). The model computes edge signals as weighted log luminance ratios. It was previously used to fit psychophysical brightness data (Rudd and Arrington 2001; Rudd and Zemach 2004) on the effects of variable annulus luminance and width in displays similar to those used in the annulus-change condition of the Kinoshita–Komatsu study. To adapt the Rudd et al. version of the contrast model to the current context, we implemented half-wave rectification of the input signals, such that there were four inputs (Fig. 1). Two inputs represented *polarity-specific* signals from the inner border, whereas the other two represented *polarity-specific* signals from the outer border (Fig. 1A). Each input was weighted by coefficients (w_j) that were fit by the method described below. The neural spike rate (x) was derived by adding the contributions of the four input kernels with a fifth free parameter (C) that set the baseline activation around which the inputs modulated

$$x = \left[\left(w_1 \left[\log \left(\frac{L_c}{L_{r1}} \right) \right]^+ + w_2 \left[\log \left(\frac{L_{r1}}{L_c} \right) \right]^+ + w_3 \left[\log \left(\frac{L_{r1}}{L_{r2}} \right) \right]^+ + w_4 \left[\log \left(\frac{L_{r2}}{L_{r1}} \right) \right]^+ + C \right]^+ \quad (1)$$

where L_c is the center luminance, L_{r1} is the luminance of the spatial region immediately surrounding the center (the region corresponding to the annulus in the annulus-change condition), and L_{r2} is the luminance of the region immediately surrounding region $r1$ (the region corresponding to the background in the annulus-change condition). In the center-change condition, $L_{r1} = L_{r2}$, and only the first two terms in Eq. 1 are relevant because $\log(L_{r1}/L_{r2}) = \log(L_{r2}/L_{r1}) = 0$. In the annulus-change condition, L_{r1} does not equal L_{r2} and so only

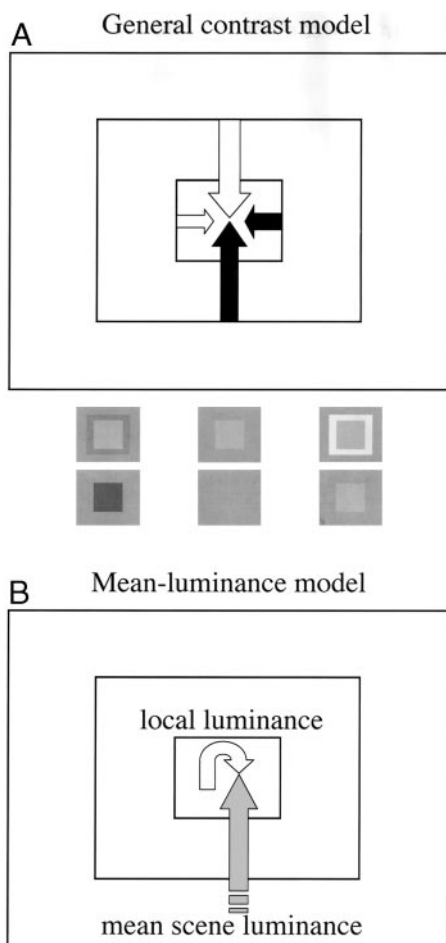


FIG. 1. Schematic illustration of the models. *A*: contrast model: the log luminance ratios computed at image borders are rectified and summed by the surface-responsive neuron. Edges of opposite polarity and the same spatial position are weighted separately. *B*: mean-luminance model: the logarithm of the local luminance is computed relative to the logarithm of the mean scene luminance, by subtraction of the weighted log mean signal from the weighted log local signal. Because the luminance values are transformed in log space, this is equivalent to computing ratios of the local and mean luminance values to the power of their respective weights (see METHODS). General contrast model has 5 free parameters, whereas the mean-luminance model has only 3 parameters. Examples of the stimuli used in the Kinoshita–Komatsu study are shown below the contrast model.

the edge pathways weighted by w_3 and w_4 are active. The positively signed brackets $[]^+$ denote half-wave rectification, meaning that spike rate could be either positive or zero, but not negative. Depending on the values of the fitted weights (w_j), the response function $f(x)$, associated with Eq. 1, can be either monotonic or nonmonotonic [where $f(x)$ represents the vector of neural responses to all stimuli in the set]. For example, all else being equal, positive values for w_1 and w_2 give rise to a V-shaped function with respect to variable L_c , as Kinoshita and Komatsu (2001) observed in some surface-responsive neurons especially during the early phases of the response (<120 ms).

We built two simplified versions of the contrast model. In one simplification, we constrained the parameters multiplying each edge polarity to equal one another. We did this separately for inner and outer edges ($w_1 = -w_2$, $w_3 = -w_4$), thereby deriving the contrast model without half-wave rectification. This constraint prevented the model from generating different slopes for opposite-edge polarities but it also reduced the number of free parameters to three, the same number as the mean-luminance model described below. In a second simplification, we constrained the contrast model such that only the

inner edge provided the inputs ($w_3 = w_4 = 0$), also giving a three-parameter model.

Half-wave-rectified luminance models

We built three versions of the luminance model. The most general form was the mean-luminance model (Fig. 1*B*) with input half-wave rectification. The other two models were derived through simplifications of this model. The mean-luminance model is based on the idea that local luminance signals are scaled by an estimate of mean luminance (e.g., Robilotto and Zaidi 2004). We modeled this theoretical idea in terms of the logarithmic ratio of the local luminance and the mean luminance, weighting each of the inputs separately by means of a power exponent. We added the input kernels, together with a third free parameter (C), to give

$$x = \left[\left[\log \left(\frac{L_c^{w_1}}{L_{mean}^{w_2}} \right) \right]^+ + C \right]^+ \quad (2)$$

where L_c and L_{mean} correspond to the luminance of the center stimulus and the mean luminance

$$L_{mean} = \frac{L_c \text{area}(c) + L_{r1} \text{area}(r1) + L_{r2} \text{area}(r2)}{\text{area}(\text{total})} \quad (3)$$

The mathematical operations embodied in Eq. 2 are equivalent to additive interactions between the logarithms of the center- and mean-luminance values, multiplied by the values of their respective weights, $w_1 \log(L_c) - w_2 \log(L_{mean})$. Equation 2 is quite flexible in the interactions it can entertain. The sign of the relationship between center- and mean-luminance values, for example, can be inverted $\log(L_{mean}^{w_2}/L_c^{w_1})$, with respect to Eq. 2, if both weights are fitted as negative values. Indeed, the relationship can also be multiplicative, as in $\log(L_c^{w_1} L_{mean}^{w_2})$ when w_1 and w_2 are positive and negative, respectively, or as in $\log(1/L_c^{w_1} L_{mean}^{w_2})$, when w_1 is negative and w_2 is positive.

We constructed two *local-luminance models*, in which only the luminance of the center patch was processed, by constraining the weight for the mean-luminance term to equal zero ($w_2 = 0$). The local-luminance models therefore had only two free parameters, and the only difference between the two versions was that we omitted the inner HWR brackets in one model and kept the brackets in the other. We expect that the local-luminance models would outperform the mean-luminance model in the case of Type 1 neurons, but not Type 2 and 3 neurons because the classification as Type 1 implies that these neurons encode only local luminance.

Fitting

We fit the models to data from each neuron individually by means of a nonlinear least-squares optimization procedure. Fitting was done on the median values, calculated over all trials, in each of the 14 stimulus conditions. We did not fit to individual trials (or means) for the following reasons: 1) the data for some stimulus conditions were highly skewed, thereby rendering the assumption (that underlies regression) of independent, Gaussian-distributed residuals implausible; and 2) the variance associated with each condition varied considerably within a neuron, violating the assumption of uniformity of variance across conditions. Although it may be possible to deal with nonuniformity of variance (by weighting each condition, assuming the variance-stimulus relationship is predictable), our choice of regression to the medians was seen as the more conservative option. This choice is perhaps justified by the zero-mean Gaussian-distributed residuals we obtained for the vast majority of neurons.

All models usually converged well, often generating high values for the variance explained, R^2 , defined as

$$R^2 = 100 \left(1 - \frac{SS_{fit}}{SS_{total}} \right) \quad (4)$$

where SS_{fit} is the sum of squares derived from the fit and SS_{total} is the sum of squares derived from a flat line given by the mean of the fitted residuals. In instances where $R^2 < 40\%$, we attempted to obtain better fits by randomly toggling the starting parameter values. We found that, in a few cases where $R^2 \approx 0\%$, changing the starting parameter led to an excellent fit. However, these cases were rare. We always took pains to obtain convergence solutions that represented global, rather than local, minima.

Performance analysis using Akaike's information criterion

We analyzed the performance of each model, that is, the goodness of fit relative to the number of parameters, using Akaike's information criterion (AIC) with sample-size correction (AIC_c). Although the AIC approach is certainly not new (Burnham and Anderson 2002), only in relatively recent times has the method begun to be applied in certain scientific contexts, such as neuroscience (Averbeck and Lee 2003; Elder and Sachs 2004; Schall et al. 2004) and phylogenetics (Posada and Buckley 2004). The core idea of the approach is to estimate the "loss of information" that occurs when one attempts to construct a model of reality. The measure of information loss consists of a mathematical term estimating the goodness of fit to a data set (e.g., sum of squares) and a term estimating the effect of the number of estimated parameters (i.e., complexity). In this sense, AIC embodies a statistical principle of parsimony. Formally, we have

$$AIC_c = N \ln \left(\frac{SS_{fit}}{N} \right) + 2K + \frac{2K(K+1)}{N-K-1} \quad (5)$$

where N is the number of data points, SS_{fit} is the fitted sum of squares, and K is the number of fitted model parameters. Generally speaking, the smaller the value of AIC_c the better the model has performed. By comparing AIC_c values for the i th model to a comparison model (C), as in

$$\Delta AIC_c^i = AIC_c^i - AIC_c^C \quad (6)$$

and computing the ratio of these differences relative to the sum of all the models (R = number of models), one obtains the relative probabilities of each model being correct, also known as Akaike's weights

$$P_i = \frac{e^{-0.5(\Delta AIC_c^i)}}{\sum_{r=1}^R e^{-0.5(\Delta AIC_c^r)}} \quad (7)$$

For comparison, we also compute a second criterion, known as the Bayesian information criterion (BIC)

$$BIC = N \ln \left(\frac{SS_{fit}}{N} \right) + K\delta \ln(N) \quad (8)$$

where $\delta = 2.5$ represents a factor correcting for small sample size (Ball 2001). An analogous computation underlies the calculation of relative probabilities associated with the BIC method. A detailed discussion and comparison of the AIC and BIC approaches are provided in Burnham and Anderson (2002).

The general AIC approach has several advantages over tests conventionally used to compare models with different numbers of parameters (Burnham and Anderson 2002). Of particular interest here, the AIC method is valid even when models are not "nested"—that is, when they cannot be derived directly from one another, as is the case with the contrast and luminance models examined here. Additionally, the AIC approach does not depend on arbitrary critical (α) values for accepting or rejecting hypotheses and does not require adjustments for multiple comparisons of the sort familiar in conventional statistical inference (e.g., Bonferroni correction). [General discussions of the

problems associated with conventional methods of statistical inference can be found elsewhere (Goodman 1999a,b; Sterne and Smith 2001)]. The AIC approach also allows one to compute evidence ratios with selected models (ratios of relative probabilities of each model being correct) or to add together the relative probabilities associated with specific models to examine the importance of parameters common to the selected models. We make particular use of the additive property in our analysis to compare the joint relative probabilities associated with the local- and mean-luminance models.

In common with conventional methods, the AIC approach depends on the assumption that model residuals are Gaussian-distributed with zero mean. We tested this assumption for all model fits using the D'Agostino–Pearson test for skewness and kurtosis, and the Student's t -test for differences of the mean residuals from zero, respectively. In only a few isolated cases did the P values associated with either test fall to <0.05 . These instances are discussed in the text, without being dismissed outright (because P values of <0.05 hold no privileged status).

Simulation methods

All simulations were performed on an Apple Mac G5 dual 2.0Gh machine using software implemented in Matlab (version 7.0.4, The MathWorks). For the mean-luminance model, we assumed that the stimulus was a 129×129 lattice of luminances [in candelas per square meter (cd/m^2)], with a central square of 41×41 pixels and an annulus of 101×101 pixels on which the square was superimposed (the contrast model, being agnostic to stimulus area, did not require this assumption). The dimensions of these stimuli conformed to the average stimulus dimensions used in the Kinoshita–Komatsu study.

RESULTS

Examples of model fits

We now analyze the data of Kinoshita and Komatsu (2001) using the modeling framework detailed above. In this section, we limit ourselves to showing example fits obtained with the most general forms of the contrast and luminance models because these provided the best fits. Figure 2A shows the responses of a neuron classified as Bright Type 3, along with the best-fitting function, $f(x)$, with 95% confidence intervals (CIs), of the contrast model. This corresponds to the conditions in which the central patch changed luminance but the background luminance (dashed vertical line) remained constant (*center-change* condition). The error bars for each data point represent the first and third quartiles associated with the median for that point. The fitted spike rates are a bit below the data points when the square is darker than the background (dashed horizontal line represents isoluminance), meaning that the model predicts slightly less ongoing activity than observed. For both model and data, the spike rate increases linearly (in log space) as the square's luminance increases above the background luminance. The difference in slopes of the two components of the model response function arises from different weightings of the opposite contrast polarities. That is, the weight associated with the decremental inner edge (square darker than the background) is small ($w_2 = 1.32 \pm 5.7$, the latter value being the 95% confidence interval on the parameter estimate), whereas the weight associated with the inner incremental edge is large ($w_1 = 24.26 \pm 4.01$; square brighter than the background).

The scenario is more complicated (Fig. 2B) when the luminance of the square is kept constant (dotted vertical line) and

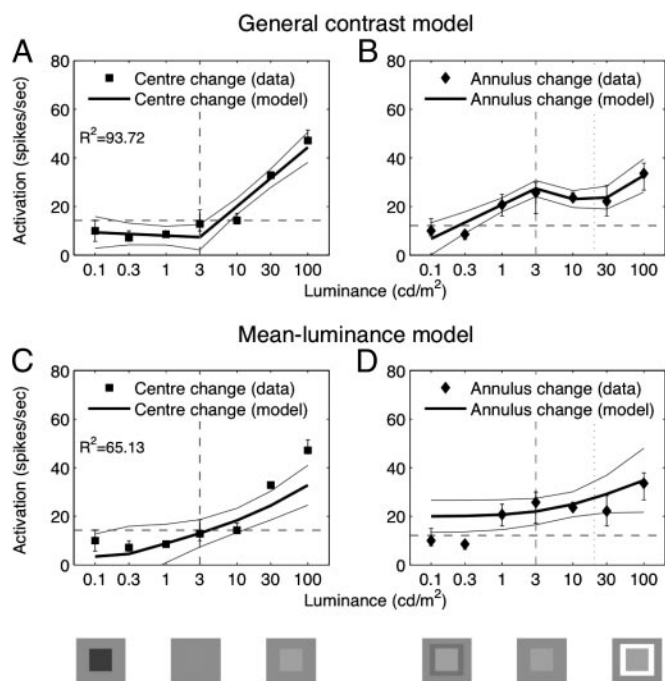


FIG. 2. One example of fits generated by contrast and mean-luminance models for a Type 3 Bright neuron. *A*: fits (thick gray line) and 95% confidence intervals (thin gray lines) of contrast model in the center-change condition. Each data point represents the neuron's median firing rate over trials, with 1st and 3rd quartiles indicated by error bars. Vertical dashed line represents the (constant) luminance of the background, whereas the horizontal dashed line represents the actual neuron's median firing rate when presented with only the background. *B*: contrast fit in the annulus-change condition. Dashed vertical line represents background luminance; the dotted vertical line is the center luminance. *C*: similar plot for the mean-luminance model in the center-change condition. *D*: fit of the mean-luminance model in the annulus-change condition. Figure illustrates that, for this neuron, the contrast model fits the data better ($R^2 = 93.72$) than the mean-luminance model ($R^2 = 65.13$). Icons below illustrate the general form of the stimuli and do not correspond directly to any of the stimulus conditions.

the luminance of the surrounding annulus changes (*annulus-change* condition). In this condition, the annulus is itself surrounded by a background surface of constant luminance (dashed vertical line), meaning that there is an inner and an outer border in the image. At the lowest annulus luminance values, the inner incremental weight is active because the annulus is much darker than the center. At the same time, the weight associated with the outer decremental edge is large and negative ($w_4 = -38.23 \pm 4.23$), which, combined with the large contrast ratio between annulus and the background, generates strong suppression. As this contrast decreases, the suppression declines and there is a steep increase in spike rate up until the point where the annulus and background are isoluminant. When the annulus becomes brighter than the background, there is a sudden dip in the model response function. This occurs because the contrasts associated with the inner and outer borders are both very small. Thus even though the inner and outer incremental weights ($w_3 = 16.05 \pm 3.64$) are positive, the small contrast ratios lead to a dip. As the annulus luminance increases above the center luminance, the inner edge becomes a weakly weighted decrement, which, when combined with the strongly weighted outer incremental edge, results in a secondary peak in the response function at the highest annulus luminance.

As expected of a model with more degrees of freedom, the fit for the contrast model ($R^2 = 93.72$) was better than that for the mean-luminance model ($R^2 = 65.13$). As we demonstrate in the following section, this fit is sufficiently better to justify the two extra parameters in the contrast model. In other words, the data strongly support the contrast model over the mean-luminance model. The fit associated with the mean-luminance model is shown in Fig. 2, *C* and *D*. The shape of the response function in the center-change condition arises as follows. Both the weighted center luminance ($w_1 = 7.98 \pm 6.51$) and weighted mean luminance ($w_2 = 12.08 \pm 9.80$) are small at the lowest center-luminance values. Because both weights are positive, the interaction between the two input signals is multiplicative, resulting in an increase in spike rate with center luminance. In the annulus-change condition, the center luminance remains constant, meaning that only the weighted mean-luminance signal varies. Because only one input source increases, the response function increases more slowly than that in the center-change condition.

A second example, a Dark Type 2 neuron, is shown in Fig. 3. The fit associated with the contrast model is only slightly better ($R^2 = 93.91$) than that associated with the mean-luminance model ($R^2 = 92.47$). In this instance, our performance analysis (see following text) indicates that the mean-luminance is more likely to be correct because it achieves a comparably good fit with fewer parameters. In the present example, the fitted response functions are decreasing in the center-change condition and increasing in the annulus-change condition. The explanations of the functions are similar to those given above. With respect to the contrast model, the main difference is that the outer edge in the annulus-change condition has only a relatively weak effect. In the case of the

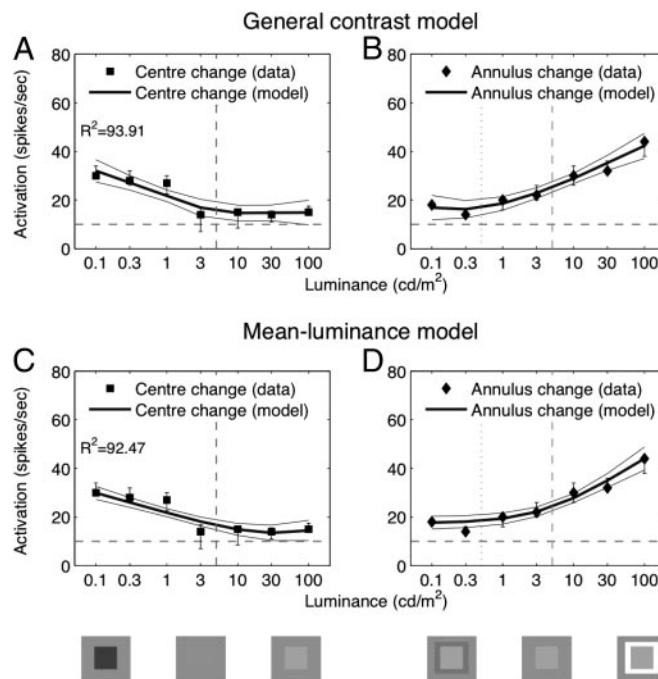


FIG. 3. Example of fits generated for a Dark Type 2 neuron. *A* and *B*: representation of the contrast-model fit. *C* and *D*: representation of the fit for the mean-luminance model. Again fit is better for the contrast model but the mean-luminance model actually performs better because it has fewer parameters. See RESULTS for details.

mean-luminance model, the weighted center luminance is negative, whereas the weighted mean luminance is positive.

Comparison of model fits

The variance explained (R^2) values for all fitted neurons are shown in separate histograms for each model in Fig. 4. Each panel also shows the breakdown of fits across the three classified types of neurons in Kinoshita and Komatsu (2001). The contrast model (Fig. 4A) generated far better fits than the mean-luminance model (Fig. 4B). The median fits over the entire population were 73 and 87% for the mean-luminance and contrast models, respectively. The contrast model generated the better fit in 60/67 neurons (90%), with a mean improvement of 15.8% associated with these 60 neurons. In 64% of neurons, fits associated with the contrast model exceeded 80%, whereas the mean-luminance model performed similarly in only 37% of neurons. Interestingly, the quality of the fits do not appear to differ substantially with the Kinoshita–Komatsu classification of RF type for either model. We now turn to the question of whether the extra variance explained by the contrast model justifies the need for two extra free parameters.

Comparison of model performance

We analyzed the performance of the general contrast and mean-luminance models using Akaike's corrected information criterion (see METHODS), a technique that trades off fit quality against number of parameters to give the probability of a given model being correct. This analysis was carried out for the entire population of 67 surface-responsive neurons. Figure 5A shows a histogram of the proportions of neurons versus the relative probabilities of the mean-luminance model being correct (the corresponding graph for the contrast model is simply Fig. 5A with left–right reversal). Relative probabilities are represented in percentages (partly to underline that our relative probabilities should not be interpreted in the classical statistical sense). The bins are 10% units wide. As a guide, we shall

interpret frequencies in the 90–100% bin as providing relatively strong evidence in favor of the mean-luminance model, with values in the 0–10% bin providing relatively strong evidence in favor of the contrast model. We emphasize, however, that such percentiles do not represent *arbitrary* statistical criteria for accepting or rejecting either model. The figure clearly shows that the mean-luminance model is favored in around 50% of neurons (34/67 neurons in the 90–100% bin, of which 18/67 fall in a 99–100% bin), with the contrast model performing well in only about 10% of neurons (6/67). In the remaining cases, there is no strong evidence in favor of either model. Similar results obtain using the BIC method (Fig. 5B). The better performance of the mean-luminance model can be traced to the fact that it has two fewer free parameters than the contrast model and so is penalized less in the calculation of relative probabilities in both the AIC and BIC analyses. For simplicity, we restrict the remainder of our analysis to the AIC method.

Because the validity of our performance analysis depends on the assumption of Gaussian-distributed residuals with zero mean, we checked that all neurons met these criteria (see METHODS). We found that in no case did the means of the residuals differ from zero. In six instances, the residuals associated with the mean-luminance model were found to be significantly non-Gaussian at $\alpha < 0.05$. Only one of these cases corresponded to a neuron deemed highly likely to be correct (90–100% bin). Likewise, there were seven cases of non-Gaussian residuals associated with the contrast model and only one such instance related to a neuron deemed highly likely to be correct (0–10% bin). Setting the statistical threshold at $\alpha < 0.01$, we found that, for both models simultaneously, only four neurons did not fulfill the Gaussian requirement. Thus the results of our analysis are not greatly affected by mild violations of the assumptions underlying the analysis.

Simplifying the contrast model

Because of the flexibility of AIC approach, we were able to simplify both the contrast and mean-luminance models and to

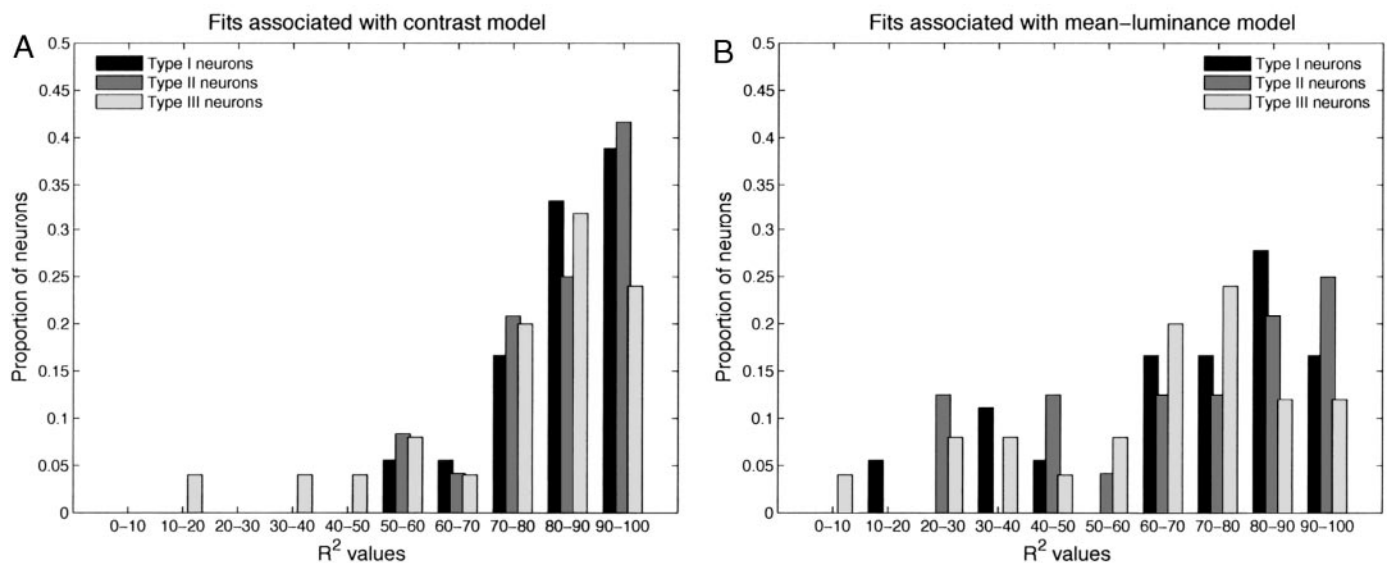


FIG. 4. Histograms of the fits associated with the general contrast and mean-luminance models. A: contrast model generated excellent fits in most cases. B: mean-luminance model generated poorer fits on average.

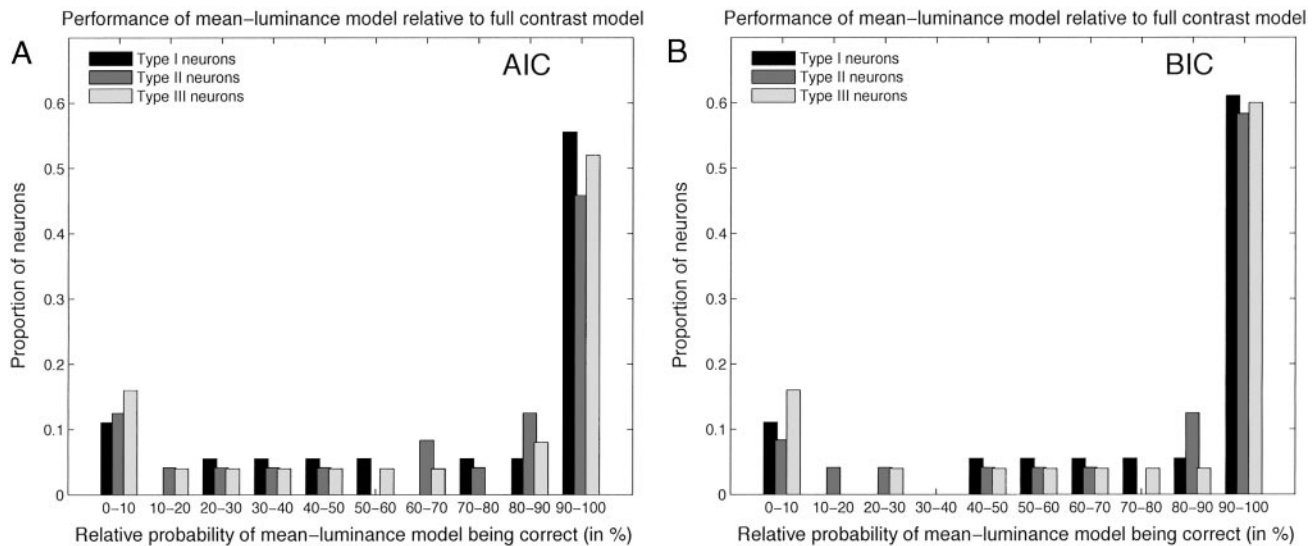


FIG. 5. Comparison of general contrast and mean-luminance models using Akaike's information criterion (AIC) and Bayesian information criterion (BIC). *A*: with the AIC method, the mean-luminance model convincingly outperforms the contrast model in nearly 50% of neurons (90–100% bin), whereas the contrast model performs similarly in only about 10% of neurons (0–10% bin). Better performance of the mean-luminance model can be traced back to the fact that it has 2 fewer parameters. *B*: BIC method produces similar results. We present the remaining results using the AIC method.

make multiple comparisons between various models without the constraints associated with classical statistical analyses. (Note that classical F-test comparisons between the luminance and contrast models are not valid, in any case, because these models are not nested.) We implemented two simplified versions of the general contrast model (see METHODS). We then fit these constrained models to the entire data set and calculated the combined relative probabilities of these models being correct relative to the mean-luminance model. We found that the performance of the mean-luminance model far exceeded that of the two constrained contrast models (Fig. 6). The performance of the constrained model without half-wave rectification (Fig. 6*A*) was roughly the same as that of the general contrast model (Fig. 5). The performance of the other constrained model, in which only the inner edge contributed to the response, was worse than that of the general contrast model for Type 1 and Type 3 neurons (Fig. 6*B*). The constrained contrast

model improved slightly in performance for Type 2 neurons, however.

Simplifying the mean-luminance model

We also implemented two simplified versions of the mean-luminance model and compared the performance of these models against that of the mean-luminance model. In these simplified models, the weight associated with the mean-luminance input was set to zero. We therefore refer to these simplified models as *local-luminance models*. The only difference between the two local-luminance models was the absence of half-wave rectification of the input signal in one model. The consequence of omitting the HWR bracket is to allow the input to become negative. We added the relative probabilities associated with the two local-luminance models (addition of relative probabilities is possible within the AIC framework) and

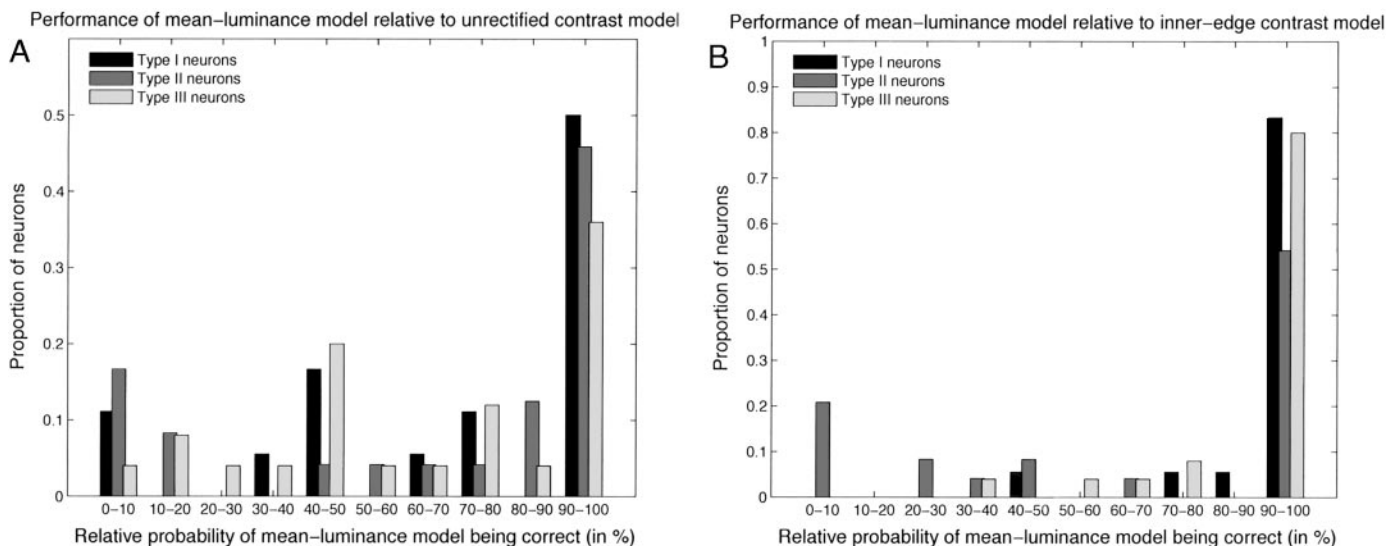


FIG. 6. Comparisons between two constrained contrast models and the mean-luminance model. *A*: unrectified version of contrast model performs about the same as the general contrast model. *B*: mean-luminance model completely outperforms the inner-edge contrast model (note the different scale).

compared these values against the relative probabilities (corrected by a factor of two) associated with the mean-luminance model.

We found that the local-luminance models convincingly outperformed the mean-luminance model in around 30% of Type 1 and Type 2 neurons (Fig. 7). These results are somewhat surprising because one may have expected that all Type 1 neurons (and no Type 2 neurons) would be better explained by the local-luminance models. The mean-luminance model, by comparison, performed very well in about 50% of Type 2 neurons and 20% of Type 3 neurons. We are led to conclude that, for many neurons originally classified as Type 3 (and to a lesser extent, those classified as Type 2), the processing of local luminance alone provides an adequate quantitative description of neuronal response profiles. Taken together with the poor overall performance of the contrast models, the present analysis suggests that the majority of surface-responsive neurons process local luminance (together with mean luminance in many cases).

Are the fitted parameters functionally interpretable?

We checked whether the estimated parameter values from our analysis of the mean-luminance model could be interpreted physiologically. Figure 8 shows the best-fitting parameters and associated 95% confidence intervals. Importantly, across the entire population of neurons (j), we found strong correlations between the parameters (w_1^j and C^j) common to the mean-luminance model and the two local-luminance models ($r^2 > 0.89$, $P < 0.0001$, in all cases). Thus studying the parameter values derived from the mean-luminance model is meaningful for the majority of neurons. In Fig. 8, the different panels represent w_1^j , w_2^j , and C^j , respectively. The color of the background encodes the neuron type. We suggest that the weighting parameters (w_1^j and w_2^j) find a natural physical interpretation in

terms of excitatory and inhibitory weightings of the input sources to neurons. The interpretation of C^j , however, seems more difficult. For example, C^j could represent spontaneous firing rates, in which case we would expect C^j to be always positive. Figure 8 indicates that this was not always the case. Another problem with this interpretation is that many neurons are likely to process local-luminance information, meaning that accurate estimates of spontaneous firing rates must come from recordings in complete darkness. The default (baseline) conditions in Kinoshita and Komatsu (2001), however, generally involved showing animals uniform gray stimuli on the experimental display. Thus it may be that C^j represents the combination of spontaneous firing rates and the influence of the background luminance stimuli. Another possibility is that C^j represents a factor analogous to the relationship (Carandini et al. 2000) between resting membrane potential (RMP) and spiking threshold (ST). If RMP is above ST, on the one hand, a neuron exhibits positive spontaneous firing rates. If RMP is below ST, on the other hand, a neuron requires additional input excitation to overcome the ST. According to this interpretation, C^j represents the value of ST relative to RMP for each neuron.

Does the luminance approach provide any new insights into the functional properties of surface coding in visual cortex? To answer this question, we plotted the weights w_1^j and w_2^j against each other (Fig. 8D). This enabled us to examine the relative contribution of local- and mean-luminance to the firing rate of each neuron. We found a significant positive linear relationship between w_1^j and w_2^j for bright neurons ($r = 0.67$, $P < 0.0001$), and a nonsignificant linear relationship for dark neurons ($r = 0.36$, $P = 0.15$). The population as a whole exhibited a V-shaped distribution, with bright neurons to the right side of the zero value for the local-luminance weight and dark neurons to the left. Here we focus only on bright neurons. When the local-luminance weight is zero ($w_1^j = 0$), surface-responsive neurons encode the weighted mean log luminance, as in

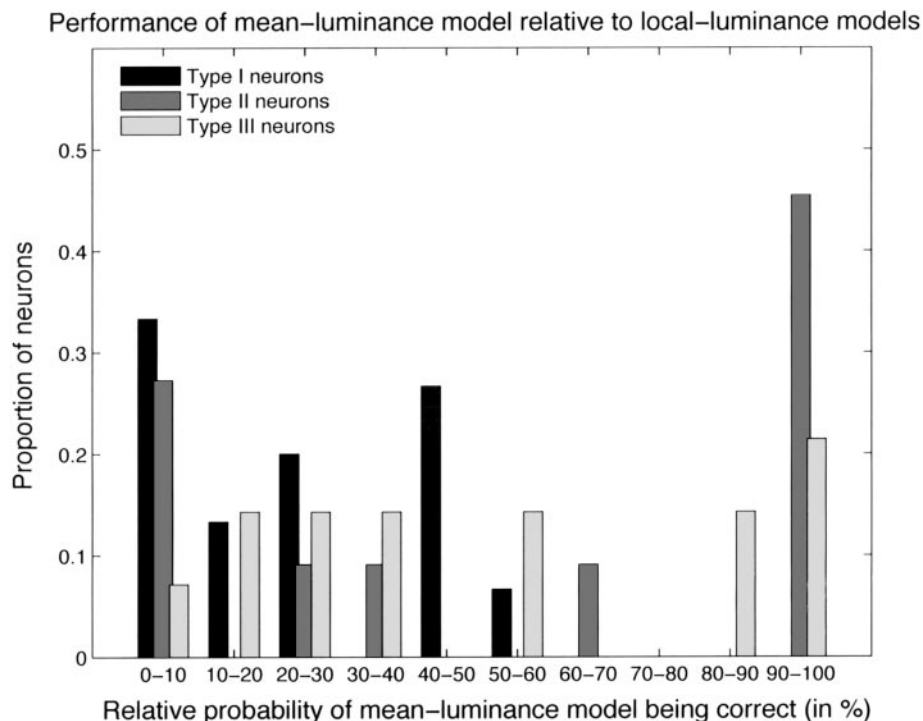


FIG. 7. Comparison between local- and mean-luminance models indicates that the mean-luminance model performs poorly for most Type 1 neurons. Although nearly 50% of Type 2 neurons and 20% of Type 3 neurons are highly consistent with the mean-luminance model, a surprisingly large proportion of these neurons are reasonably well described by the local-luminance models. These quantitative results suggest that many Type 2 and 3 neurons were incorrectly classified in the Kinoshita-Komatsu study.

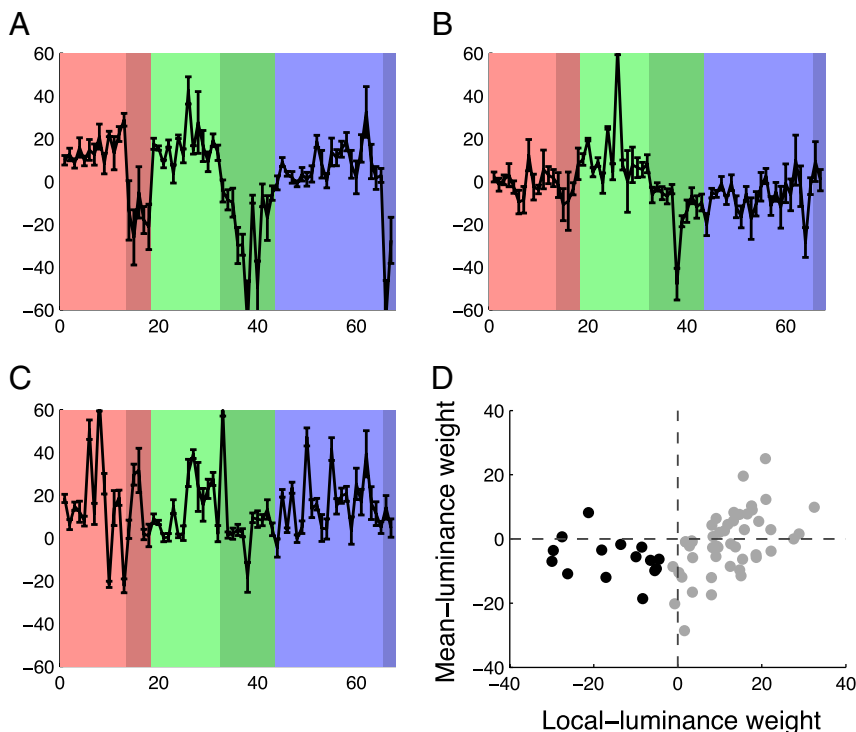


FIG. 8. All fitted parameters for the mean-luminance model for each neuron. Weights associated with the local-luminance signal (A) and the mean-luminance signal (B). C: additive constants. Shaded red, green, and blue regions correspond to Types 1, 2, and 3 neurons, respectively. Lighter shading represents Bright neurons, whereas the darker regions indicate Dark neurons. Weighting parameters are readily interpretable in terms of excitatory and inhibitory inputs to neurons, whereas the additive constant is more difficult to interpret. D: scatterplot relating local- and mean-luminance weights. Different functional classes are interpreted in terms of different combinations of local- and mean-luminance weights. See text for further discussion.

$\log(L_{mean}^{w_2})$. As the value of the local-luminance weight becomes more positive ($w_1^j \rightarrow \infty$), we first pass through a region of parameter space where local- and mean-luminance terms are positive and negative, respectively, as in $\log(L_c^{w_1} L_{mean}^{w_2})$. These neurons would correspond to Type 3 neurons in the Kinoshita–Komatsu classification scheme. As noted previously, however, strong AIC evidence in favor of the Type 3 classification emerged in only a few neurons. One possible functional interpretation of neurons exhibiting strong evidence for positive and negative local- and mean-luminance weights is that, in reality, these neurons sum luminance signals over the entire visual field, with greater weight assigned to local luminance signals. As w_1^j increases further, the mean-luminance weights first approach zero ($w_2^j \rightarrow 0$), corresponding to the local-luminance coding regime, as in $\log(L_c^{w_1})$, before taking on positive values ($w_2^j \rightarrow \infty$), thereby encoding weighted local luminance relative to weighted mean luminance, as in $\log(L_c^{w_1}/L_{mean}^{w_2})$. The latter neurons may partially discount illumination through ratio processing (Type 2 neurons), although the efficiency of the discounting will depend on the precise values of w_1^j and w_2^j : discounting is 100% efficient when $w_1^j = w_2^j \neq 0$. To summarize, our analysis suggests that most neurons encode either local or mean luminance and, in some instances, local luminance relative mean luminance. These functional types would therefore appear to provide useful information about complementary aspects of the stimulus.

DISCUSSION

In this study, we have developed models to examine whether the known properties of surface-responsive V1 neurons (Kinoshita and Komatsu 2001) could be better explained by assuming processing of luminance or contrast signals. Our results indicate that, even though the full contrast model provides the better fits, the mean-luminance model performs

better in the majority of neurons. The full contrast model clearly performs better in only a small minority of neurons. Simplification of the mean-luminance model, but not the full contrast model, leads to improvements in performance in a sizable proportion of neurons. Not all neurons are well fit by any of the tested models, however, and in some instances the data do not strongly support one or another model. To the extent that we acknowledge that all models are necessarily wrong—that is, they all fall short of describing reality—we view our methods and results as a useful guide for interpreting experimental data on surface-responsive neurons (Hung et al. 2001, 2002; Peng and Van Essen 2005; Roe et al. 2005). Because our results depend on a statistical technique that appears to be relatively unfamiliar in visual neuroscience, we first briefly discuss the approach.

Akaike's information criterion and model selection

Determining how well a model describes reality—or selecting between competing models of reality—is a fundamental problem in science. The approach used herein—Akaike's information criterion, or AIC—is based on considerations from information theory (Burnham and Anderson 2002). Briefly, AIC measures the amount of information lost when a model is used to approximate reality. Of a candidate set of models, the model that minimizes the loss of information is deemed most likely to be correct. The loss of information is quantified in the trade-off between goodness of fit and number of free parameters (see METHODS). Importantly, AIC is *not* derived under the assumption that the true model is included in the candidate set of models.

The AIC approach is becoming increasingly popular in the biological sciences, largely because of its simplicity and flexibility (Elder and Sachs 2004; Posada and Buckley 2004). Multimodel analyses of the type performed herein, for exam-

ple, are not possible with conventional statistical approaches, such as the F-ratio test (Burnham and Anderson 2002). The present application represents one of the first uses of AIC in the context of modeling neurophysiological data (Averbeck and Lee 2003; Schall et al. 2004). Averbeck and Lee (2003), for example, used a simpler version of the AIC approach (one not corrected for sample size) in their study of neural coding in the supplementary motor area of the rhesus monkey.

A reappraisal of surface coding in V1

Kinoshita and Komatsu (2001) classified surface-responsive neurons according to the slopes of their response functions in center- and annulus-change conditions. We adopted a complementary approach in our analysis, asking whether neurons' responses were better explained by luminance or contrast information, regardless of the respective slopes of the response functions. Our analysis indicates that neurons classified as different based on analysis of response slopes may, in fact, share hidden similarities. Neurons for which we found strong evidence of contrast processing, for example, were of both the Type 2 and Type 3 varieties. Conversely, we found that only 30% of neurons classified by Kinoshita and Komatsu (2001) as Type 1 were better explained by our local-luminance models, relative to the mean-luminance model (although no Type 1 neurons were better explained by the mean-luminance model than the local-luminance models). We conclude that, to draw meaningful functional conclusions concerning the information processed by surface-responsive neurons in the Kinoshita–Komatsu experiments, one needs to take into account more than the slopes of the response functions.

Distinguishing between contrast and luminance responses

Roe et al. (2005) examined surface-responsive neurons using stimuli well suited to delineating between contrast and luminance responses (see also Hung et al. 2001). Their stimuli consisted of a bipartite field in which left and right halves modulated in counterphase over time, keeping mean luminance constant. Either the left or right half of the stimulus was placed over the mapped local RF of a neuron. In one condition, the luminance values of the entire left and right hemifields modulated in time (real luminance change). In a second condition, the authors used Cornsweet stimuli to modulate only luminance values near the border—a stimulus that elicits illusory brightness filling-in in humans—while keeping local luminance within the RF, and also mean scene luminance, constant.

The findings of Roe et al. (2005) are in agreement with our conclusion that the vast majority of surface-responsive neurons process luminance information (note that the stimuli of Roe et al. cannot be used to distinguish local- and mean-luminance models because mean luminance was always constant). These authors found that around 50% of sampled V1 and V2 neurons were significantly modulated by local-luminance changes (i.e., surface responsive). In comparison, no surface-responsive V1 neurons, and only around 10% of surface-responsive V2 neurons, were significantly modulated by the Cornsweet stimulus. Optical imaging revealed significant activation in V2 thin stripes for both real and illusory brightness changes, although no significant signal was obtained in V1 for either stimulus type. Roe et al. concluded that the computations underlying surface brightness are likely to occur in V2 but not in V1.

The results of Roe et al. (2005) support the generality of our conclusion that luminance processing predominates over contrast integration in V1 neurons. This point is of particular importance because the stimuli used by Roe et al. differed in key ways from those of Kinoshita and Komatsu (2001). The luminance stimuli of Roe et al. varied sinusoidally in time, and the authors' analyses were based on the spike rates derived over the entire presentation period. In contrast, the stimuli of Kinoshita and Komatsu remained static over the entire presentation period, and our analyses were based only on the latter part of the response. It remains to be seen whether application of our analysis to V2 neurons would support contrast integration.

Tuning for luminance stimuli

Peng and Van Essen (2005) reported that around 10–30% of surface-responsive neurons in macaque V1 and V2 are tuned for luminance stimuli in a manner analogous to the way edge-responsive neurons are tuned to spatial frequency. In the context of the experiments of Kinoshita and Komatsu (2001), luminance tuning corresponds to peak firing rates at luminance values away from the maximum or minimum values used in the experiments. Although we did not test any models that incorporate luminance tuning, we observed informally that instances where both models fit the data poorly were largely a result of nonmonotonic relationships between firing rate and center (or annulus) luminance, as would be expected with luminance tuning. The methods developed herein could be naturally extended to quantitatively assess evidence for various forms of luminance tuning in future modeling studies.

Roles of contrast and luminance

This paper began with an overview of the two main stimulus cues in achromatic surface perception: contrast and luminance. We had expected to find strong evidence in favor of contrast integration in many cortical neurons because this notion is at the core of many models of surface perception (Land and McCann 1971). Psychophysical evidence points to a critical role for contrast in determining surface brightness (Davey et al. 1998; Hong and Shevell 2004a,b; Paradiso and Nakayama 1991; Rossi and Paradiso 1996; Rudd and Arrington 2001; Rudd and Zemach 2004; Shapiro et al. 2004). Yet, as indicated in our introductory remarks, contrast processing does not obviate the need for luminance processing. Indeed, theoretical studies support roles for both local luminance (Gilchrist 1999; Pessoa et al. 1995) and mean luminance (Land and McCann 1971; Robilotto and Zaidi 2004) in determining aspects of brightness and lightness perception. More generally, if no luminance information were to reach visual cortex, animals would be unable to estimate overall light level (Barlow and Verrillo 1976; Masin 2003). Previous reports of cortical neurons that respond to Ganzfeld luminance stimuli (Kayama et al. 1979; Maguire and Baizer 1982) are also consistent with the notion that both luminance and contrast play important roles in determining surface brightness. The precise nature of the putative contribution of surface-responsive neurons to brightness perception, however, remains unclear, particularly in light of the availability of alternative approaches to brightness that do not involve assumptions of spatial isomorphism (Blakeslee

and McCourt 1999; Friedman et al. 2003; Zhou et al. 2000). Consistent with the present analysis, and with approaches eschewing spatial isomorphism, a recent fMRI study (Cornelissen et al. 2006) has shown that temporal changes in local luminance, but not brightness changes induced through temporal modulation of a surround field, are correlated with retinotopic activity in early human visual cortex.

Limitations and additional considerations

Our analysis is based on responses obtained (for most neurons) in the 520- to 1,020-ms epoch after stimulus onset. How then might we reconcile the temporal discrepancy between the latency of neural responses and psychophysical data indicating that human brightness percepts emerge after about 120 ms (Davey et al. 1998; Paradiso and Nakayama 1991; Rossi and Paradiso 1996) or even earlier (Mccourt and Foxe 2004)? One answer is that the temporal discrepancy is not as great as it first appears. It is clear, for example, from Figs. 3 and 8 of Kinoshita and Komatsu (2001), that responses characteristic of surface coding, such as polarity selectivity and the modulatory effects of annuli, actually emerged at around 120–220 ms in most neurons. Thus our analysis of the 520- to 1,020-ms epoch may actually generalize to earlier epochs that appear more consistent with classical psychophysical estimates of the time course of brightness perception (Davey et al. 1998; Paradiso and Nakayama 1991; Rossi and Paradiso 1996). A second answer is that recent psychophysical evidence indicates that temporal aspects of brightness perception may consist of separate contrast and luminance components with different time courses. Shapiro et al. (2004), for example, provide evidence to indicate that luminance signals primarily determine brightness at temporal frequencies around 1 Hz, whereas contrast signals primarily determine brightness at higher temporal frequencies. The relatively sluggish luminance-based responses studied here would therefore appear to fit well with the slow luminance component of brightness perception. One potential explanation for the sluggish nature of these responses is that local-luminance signals must be extracted through cortical computations (Neumann 1996) from the combined luminance/contrast signals encoded by LGN input neurons (e.g., Barlow and Levick 1969; Mante et al. 2005; Rossi and Paradiso 1999). As indicated previously, luminance signals may also contribute to the anchoring of lightness percepts (Gilchrist et al. 1999). Because the temporal properties of lightness anchoring are not known, it remains possible that the time course of luminance responses in visual cortex may be consistent with anchoring. None of these speculations, however, sheds light on the manner in which luminance and contrast signals might combine to determine brightness and lightness within a framework that does not depend on spatial isomorphism.

Another potential limitation of the present study concerns the use of multiunit recordings in our analysis. Of the recordings in the Kinoshita and Komatsu (2001) study, 30/76 (40%) were obtained under conditions where it was not possible to isolate single neurons. This may have led to an averaging-out of the response properties of the contributing neurons, leading to uncertainties concerning the classification of recordings into functional types. Recordings classified as Type 1, for instance, may actually have arisen through averaging of individual Type 2 and Type 3 neuronal responses. This is because pooling

spikes from Type 2 and Type 3 neurons, which respond with opposite sign to changes in annulus luminance, would tend to flatten out the response function in the annulus-change condition, thereby making multiunit recording traces appear more like Type 1 “neurons.” The use of multiunit recordings in our study probably does not affect our main conclusion that the mean-luminance model outperforms the contrast model because identical results were obtained for all functional classes. It is nonetheless possible that the comparison between local- and mean-luminance models may have been partially distorted by the use of multiunit traces. Table 2 of Kinoshita and Komatsu (2001), however, shows that only 12 of 30 multiunit recordings were classified as Type 1, implying that multiunit recordings largely agree with traces obtained from single neurons.

We conclude that no single model of surface coding captures the heterogeneous nature of cortical surface computations. Our theoretical approach, in which log luminance ratio processing is combined with half-wave rectification, provides a simple and novel mathematical framework for examining specific variants of surface-coding models. The challenge for future research will be to further refine our understanding of the myriad cortical mechanisms underlying surface coding to link them to brightness and lightness perception.

ACKNOWLEDGMENTS

We thank Professors Kinoshita and Komatsu for kindly providing the data on which this study was based. The criticisms of four reviewers led to substantial improvements in several aspects of the manuscript.

GRANTS

This work was supported by the Cognition Program of the Netherlands Organization for Scientific Research Grant 051.02.080.

REFERENCES

- Arend LE and Spehar B.** Lightness, brightness, and brightness contrast: 1. Illuminance variation. *Percept Psychophys* 54: 446–456, 1993a.
- Arend LE and Spehar B.** Lightness, brightness, and brightness contrast: 2. Reflectance variation. *Percept Psychophys* 54: 457–468, 1993b.
- Averbeck BB and Lee D.** Neural noise and movement-related codes in the macaque supplementary motor area. *J Neurosci* 23: 7630–7641, 2003.
- Ball RD.** Bayesian methods for quantitative trait loci mapping based on model selection: approximate analysis using the Bayesian information criterion. *Genetics* 159: 1351–1364, 2001.
- Barlow HB and Levick WR.** Changes in the maintained discharge with adaptation level in the cat retina. *J Physiol* 202: 699–718, 1969.
- Barlow RB Jr and Verrillo RT.** Brightness sensation in a ganzfeld. *Vision Res* 16: 1291–1297, 1976.
- Bindman D and Chubb C.** Brightness assimilation in bullseye displays. *Vision Res* 44: 309–319, 2004a.
- Bindman D and Chubb C.** Mechanisms of contrast induction in heterogeneous displays. *Vision Res* 44: 1601–1613, 2004b.
- Blakeslee B and McCourt ME.** A multiscale spatial filtering account of the White effect, simultaneous brightness contrast and grating induction. *Vision Res* 39: 4361–4377, 1999.
- Boucard CC, van Es JJ, Maguire RP, and Cornelissen FW.** Functional magnetic resonance imaging of brightness induction in the human visual cortex. *Neuroreport* 16: 1335–1338, 2005.
- Burnham KP and Anderson DR.** *Model Selection and Multimodel Inference: A Practical Information-Theoretic Approach*. New York: Springer-Verlag, 2002.
- Carandini M and Ferster D.** Membrane potential and firing rate in cat primary visual cortex. *J Neurosci* 20: 470–484, 2000.
- Cohen MA and Grossberg S.** Neural dynamics of brightness perception: features, boundaries, diffusion, and resonance. *Percept Psychophys* 36: 428–456, 1984.

- Cornelissen FW, Wade AR, Vladusich T, Dougherty RF, and Wandell BA.** No fMRI evidence for brightness and color filling-in in early human visual cortex. *J Neurosci* In press.
- Davey MP, Maddess T, and Srinivasan MV.** The spatiotemporal properties of the Craik-O'Brien-Cornsweet effect are consistent with "filling-in." *Vision Res* 38: 2037–2046, 1998.
- Elder JH and Sachs AJ.** Psychophysical receptive fields of edge detection mechanisms. *Vision Res* 44: 795–813, 2004.
- Friedman HS, Zhou H, and von der Heydt R.** The coding of uniform colour figures in monkey visual cortex. *J Physiol* 548: 593–613, 2003.
- Gerrits HJ and Vendrik AJ.** Simultaneous contrast, filling-in process and information processing in man's visual system. *Exp Brain Res* 11: 411–430, 1970.
- Gilchrist A, Kossyfidis C, Bonato F, Agostini T, Cataliotti J, Li X, Spehar B, Annan V, and Economou E.** An anchoring theory of lightness perception. *Psychol Rev* 106: 795–834, 1999.
- Goodman SN.** Toward evidence-based medical statistics. 1: The P value fallacy. *Ann Intern Med* 130: 995–1004, 1999a.
- Goodman SN.** Toward evidence-based medical statistics. 2: The Bayes factor. *Ann Intern Med* 130: 1005–1013, 1999b.
- Grossberg S and Mingolla E.** Neural dynamics of form perception: boundary completion, illusory figures, and neon color spreading. *Psychol Rev* 92: 173–211, 1985.
- Grossberg S and Todorovic D.** Neural dynamics of 1-D and 2-D brightness perception: a unified model of classical and recent phenomena. *Percept Psychophys* 43: 241–277, 1988.
- Heeger DJ.** Modeling simple-cell direction selectivity with normalized, half-squared, linear operators. *J Neurophysiol* 70: 1885–1898, 1993.
- Helson H and Himelstein P.** A short method for calculating the adaptation-level for absolute and comparative rating judgments. *Am J Psychol* 68: 631–637, 1955.
- Hong SW and Shevell SK.** Brightness contrast and assimilation from patterned inducing backgrounds. *Vision Res* 44: 35–43, 2004a.
- Hong SW and Shevell SK.** Brightness induction: unequal spatial integration with increments and decrements. *Vis Neurosci* 21: 353–357, 2004b.
- Huang X, MacEvoy SP, and Paradiso MA.** Perception of brightness and brightness illusions in the macaque monkey. *J Neurosci* 22: 9618–9625, 2002.
- Hung CP, Ramsden BM, Chen LM, and Roe AW.** Building surfaces from borders in areas 17 and 18 of the cat. *Vision Res* 41: 1389–1407, 2001.
- Hung CP, Ramsden BM, and Roe AW.** Weakly modulated spike trains: significance, precision, and correction for sample size. *J Neurophysiol* 87: 2542–2554, 2002.
- Kayama Y, Riso RR, Bartlett JR, and Doty RW.** Luxotonic responses of units in macaque striate cortex. *J Neurophysiol* 42: 1495–1517, 1979.
- Kinoshita M and Komatsu H.** Neural representation of the luminance and brightness of a uniform surface in the macaque primary visual cortex. *J Neurophysiol* 86: 2559–2570, 2001.
- Komatsu H, Kinoshita M, and Murakami I.** Neural responses in the retinotopic representation of the blind spot in the macaque V1 to stimuli for perceptual filling-in. *J Neurosci* 20: 9310–9319, 2000.
- Komatsu H, Kinoshita M, and Murakami I.** Neural responses in the primary visual cortex of the monkey during perceptual filling-in at the blind spot. *Neurosci Res* 44: 231–236, 2002.
- Land EH.** Experiments in color vision. *Sci Am* 200: 84–94 passim, 1959.
- Land EH.** The retinex theory of color vision. *Sci Am* 237: 108–128, 1977.
- Land EH.** Recent advances in retinex theory and some implications for cortical computations: color vision and the natural image. *Proc Natl Acad Sci USA* 80: 5163–5169, 1983.
- Land EH.** An alternative technique for the computation of the designator in the retinex theory of color vision. *Proc Natl Acad Sci USA* 83: 3078–3080, 1986.
- Land EH and McCann JJ.** Lightness and retinex theory. *J Opt Soc Am* 61: 1–11, 1971.
- MacEvoy SP and Paradiso MA.** Lightness constancy in primary visual cortex. *Proc Natl Acad Sci USA* 98: 8827–8831, 2001.
- Maguire WM and Baizer JS.** Luminance coding of briefly presented stimuli in area 17 of the rhesus monkey. *J Neurophysiol* 47: 128–137, 1982.
- Mante V, Frazor RA, Bonin V, Geisler WS, and Carandini M.** Independence of luminance and contrast in natural scenes and in the early visual system. *Nat Neurosci* 8: 1690–1697, 2005.
- Masin SC.** On the determinants of surface brightness. *Psychon Bull Rev* 10: 220–223, 2003.
- McCourt ME and Foxe JJ.** Brightening prospects for early cortical coding of perceived luminance: a high-density electrical mapping study. *Neuroreport* 15: 49–56, 2004.
- Neumann H.** Mechanisms of neural architecture for visual contrast and brightness perception. *Neural Networks* 9: 921–936, 1996.
- Paradiso MA and Nakayama K.** Brightness perception and filling-in. *Vision Res* 31: 1221–1236, 1991.
- Peng X and Van Essen DC.** Peaked encoding of relative luminance in macaque areas V1 and V2. *J Neurophysiol* 93: 1620–1632, 2005.
- Pessoa L, Mingolla E, and Neumann H.** A contrast- and luminance-driven multiscale network model of brightness perception. *Vision Res* 35: 2201–2223, 1995.
- Pessoa L, Thompson E, and Noë A.** Finding out about filling-in: a guide to perceptual completion for visual science and the philosophy of perception. *Behav Brain Sci* 21: 65–144, 1998.
- Posada D and Buckley TR.** Model selection and model averaging in phylogenetics: advantages of Akaike information criterion and Bayesian approaches over likelihood ratio tests. *Syst Biol* 53: 793–808, 2004.
- Reid RC Jr and Shapley R.** Brightness induction by local contrast and the spatial dependence of assimilation. *Vision Res* 28: 115–132, 1988.
- Robilotto R and Zaidi Q.** Limits of lightness identification for real objects under natural viewing conditions. *J Vis* 4: 779–797, 2004.
- Roe AW, Lu HD, and Hung CP.** Cortical processing of a brightness illusion. *Proc Natl Acad Sci USA* 102: 3869–3874, 2005.
- Rossi AF and Paradiso MA.** Temporal limits of brightness induction and mechanisms of brightness perception. *Vision Res* 36: 1391–1398, 1996.
- Rossi AF and Paradiso MA.** Neural correlates of perceived brightness in the retina, lateral geniculate nucleus, and striate cortex. *J Neurosci* 19: 6145–6156, 1999.
- Rossi AF, Rittenhouse CD, and Paradiso MA.** The representation of brightness in primary visual cortex. *Science* 273: 1104–1107, 1996.
- Rudd ME and Arrington KF.** Darkness filling-in: a neural model of darkness induction. *Vision Res* 41: 3649–3662, 2001.
- Rudd ME and Zemach IK.** Quantitative properties of achromatic color induction: an edge integration analysis. *Vision Res* 44: 971–981, 2004.
- Schall JD, Sato TR, Thompson KG, Vaughn AA, and Juan CH.** Effects of search efficiency on surround suppression during visual selection in frontal eye field. *J Neurophysiol* 91: 2765–2769, 2004.
- Shapiro AG, D'Antona AD, Charles JP, Belano LA, Smith JB, and Shear-Heyman M.** Induced contrast asynchronies. *J Vis* 4: 459–468, 2004.
- Shapley R and Reid RC.** Contrast and assimilation in the perception of brightness. *Proc Natl Acad Sci USA* 82: 5983–5986, 1985.
- Sterne JAC and Smith GD.** Sifting the evidence: what's wrong with significance tests? *Br Med J* 322: 226–231, 2001.
- Zhou H, Friedman HS, and von der Heydt R.** Coding of border ownership in monkey visual cortex. *J Neurosci* 20: 6594–6611, 2000.